FORWARD MODELING OF INDUCED POLARIZATION IN AN ANISOTROPIC CONDUCTIVE SUBSURFACE

Weiqiang Liu, Pinrong Lin, Qingtian Lv, Institute of Geophysical and Geochemical Exploration of Chinese Academy of Geological Sciences, Langfang, PR China;
Rujun Chen, Central South University, Changsha, P.R.China;
Hongchun Yao, Ruijie Shen , Champion Geophysical Technology, Changsha, P.R.China
Hongzhu Cai, University of Utah, Salt Lake City, USA

Abstract

Induced polarization (IP) methods are effective approaches in exploration and environmental geophysics. In practice, the earth electrical conductivity shows anisotropy, which will also influence the IP response. However, only a few researches have studied this issue. In this paper, we modeled and analyzed the induced polarization response in the anisotropic conductive subsurface. The finite volume method (FVM) was used to model the 3D anisotropic resistivity model, and the maximum relative error for a vertical anisotropy two-layer model is below 1%. Then we calculated the TDIP response and FDIP response based on equivalent resistivity and Cole-Cole model respectively through taking account of anisotropic model parameters. Finally, we analyzed the IP response of a two-layer horizontal anisotropic model and a 3D cube model embedded in the horizontal anisotropic subsurface. The results suggest that anisotropy paradox phenomenon still exists in the IP forwarding modeling. Apparent IP parameters of the survey lines on the surface are different between two orthogonal directions. The anisotropy should be taken into account in practical TDIP and FDIP exploration.

Introduction

Comparing to the traditional direct current (DC) resistivity method, induced polarization methods operated in both time domain (TDIP) and frequency domain (FDIP) are more effective than resistivity alone in exploration for nonferrous metallic deposits (Xi et al., 2013; Xi et al., 2014; Liu et al., 2015; Liu et al., 2016). In practical prospecting, the electric conductivity of the earth shows anisotropic effects, which can be caused by tilted stratified rocks, parallel or vertical fracturing , specific mineral crystals, inhomogeneous sedimentation rate and so on. Currently, both forward modeling and inversion algorithms for anisotropic effect in direct current method (DC) have been studied by plenty of experts. In induced polarization exploration, ignoring anisotropy will also yield misleading results. Comparing to DC method, only a few scholars have studied the induced polarization response in the anisotropic subsurface. Zhdanov (2008) developed a new generalized effective-medium theory of induced polarization (GEMTIP) to model complex resistivity and studied the anisotropy effect in IP data. Winchen et al. (2009) investigated anisotropic complex conductivity of the two isotropic materials heterogeneous mixtures, and the Cole-Cole model was used to depict soil with bimodal textural characteristics. Kenkel et al. (2012, 2013, 2014) has done a lot of work in this area. He discussed mixing laws for anisotropic complex conductivity in layered situations, and employed a 2.5D finite element method to model and invert the anisotropic complex conductivity response. In conclusion, this anisotropy effect is being taken into account in the IP data interpretation gradually. However, because IP response of the anisotropic conductive medium is sophisticated and many parameters need to be considered, there are still many problems need to be solved.

Based on the previous researches, numerical modeling of IP response in a 3D anisotropic medium was studied in this paper. First, we applied a finite volume method (FVM) discretization and an anisotropic boundary condition to realize the 3D anisotropic resistivity forward modeling. Then we used matrix calculation to substitute the scalar calculation to calculate and analysis the TDIP and FDIP response based on equivalent resistivity and Cole-Cole model respectively. Finally, we modeled and inspected the induced polarization response for a 3D cube model in the anisotropic earth. In the future, the IP response in an arbitrarily anisotropic medium can be studied further based on the anisotropy and coordinates rotation.

3D IP Forward Modeling

The potential governing equation and boundary condition for the electrical model in direct current field or low-frequency alternating current field can be expressed as:

$$\begin{cases} \nabla\cdot(\boldsymbol{\sigma}\cdot\nabla U) = -I\delta(\mathbf{r}-\mathbf{r}_q) \\ \dfrac{\partial U}{\partial n} = 0 \qquad \in \Gamma_S \\ \boldsymbol{\sigma}\dfrac{\partial U}{\partial n} + \dfrac{|r|\cos(\vec{r},\vec{n})}{B}U = 0 \qquad \in \Gamma_\infty \end{cases} \tag{1}$$

where, $\mathbf{r}$ and $\mathbf{r}_q$ are the location of the survey point and the point current source separately. $\boldsymbol{\sigma}$ is the conductivity tensor, and,

$$|r| = |\mathbf{r}-\mathbf{r}_q| = \sqrt{(x-x_q)^2+(y-y_q)^2+(z-z_q)^2} \tag{2}$$

$$\boldsymbol{\sigma} = \begin{bmatrix} \sigma_{xx} & 0 & 0 \\ 0 & \sigma_{yy} & 0 \\ 0 & 0 & \sigma_{zz} \end{bmatrix} \tag{3}$$

$$B = \frac{1}{\sigma_{xx}}(x-x_q)^2 + \frac{1}{\sigma_{yy}}(y-y_q)^2 + \frac{1}{\sigma_{zz}}(z-z_q)^2 \tag{4}$$

A Neumann boundary condition is on the earth and air interface Γ_S, and a mixed boundary condition is on the infinite boundary Γ_∞. In order to remove the source singularity, assuming the potential and conductivity consist of two parts: anomaly and background respectively, we used the analytical solution of anisotropy half-space to replace the source item, namely,

$$\nabla\cdot(\boldsymbol{\sigma}_0\cdot\nabla U_0) = -I\delta(\mathbf{r}-\mathbf{r}_q) \tag{5}$$

Where, $\boldsymbol{\sigma}_0$ is the background conductivity tensor of the study domain. U_0 is the analytical solution for the potential calculated by the formula:

$$U_0 = \frac{I}{2\pi\sqrt{B}}\sqrt{\frac{1}{\sigma_{xx}\ \sigma_{yy}\ \sigma_{zz}}} \tag{6}$$

The finite volume method (FVM) was used to approximate the former boundary value problem. First, the model is subdivided into a number of small cell-centered hexahedron volumes surrounding each node point. Second, for each volume, the partial derivative is replaced approximately by the

difference of the potential in corresponding two boundaries according to the Gaussian divergence theorem. For example, in the volume $V_{i,j,k}$, assuming $U_{i,j,k}$ is the center node potential in this volume, and corresponding conductivity is $\sigma_{i,j,k}$, corresponding cell length is $h^x_{i,j,k}$, $h^y_{i,j,k}$, $h^z_{i,j,k}$ in three directions. For the first term of the governing equation in this volume:

$$\frac{\partial}{\partial x}(\sigma_{xx}\frac{\partial U}{\partial x}) \approx \frac{1}{h^x_{i,j,k}}[(\sigma_{xx}\frac{\partial U}{\partial x})_{i+\frac{1}{2},j,k} - (\sigma_{xx}\frac{\partial U}{\partial x})_{i-\frac{1}{2},j,k}] \tag{7}$$

And, $(\sigma)_{i-\frac{1}{2},j,k}$ is the harmonic mean conductivity of the two adjacent volumes:

$$(\sigma)_{i-\frac{1}{2},j,k} = \frac{V_{i-1,j,k} + V_{i,j,k}}{V_{i-1,j,k}/(\sigma)_{i-1,j,k} + V_{i,j,k}/(\sigma)_{i,j,k}} \tag{8}$$

Partial derivative is replaced by numerical difference, such as:

$$(\frac{\partial U}{\partial x})_{i-\frac{1}{2},j,k} = \frac{U_{i,j,k} - U_{i-1,j,k}}{(h_{i-1,j,k} + h_{i,j,k})/2} \tag{9}$$

For the research domain boundary, the potential gradient $\frac{\partial U}{\partial x}$ is replaced by the product of potential value U and an undetermined constant according to the Neumann boundary condition (2) or mixed boundary condition (3). Additionally, other terms in the governing equation are also calculated using the same numerical method. After approximating the governing equation in all the volumes and assembling them into a global matrix, a linear equations system can be obtained finally, which was solved by **Intel MKL PARDISO** in this paper. Finally, apparent resistivity can be calculated.

Many physical-mathematical principles of the IP effect were originally formulated. In actual TDIP survey, the polarizability is defined as:

$$\eta = \frac{U_s}{U_t} = \frac{U_t - U}{U_t} \tag{10}$$

U is the original voltage when the inducing current just starts, U_t is the total voltage when the time for inducing current supplying is sufficient. U_s is secondary voltage caused by the induced polarization phenomenon, which is the difference between the total voltage and original voltage. In forward modeling, we used the original resistivity ρ to calculate the primary voltage U . Then the total voltage U_t was calculated through replacing the resistivity ρ by equivalent resistivity ρ_t :

$$\rho_t = \rho/(1-\eta) \tag{11}$$

Then apparent chargeability can be calculated using surface potential. When the electrical substance is anisotropic, both the real original resistivity and real equivalent resistivity of this model are identity matrices. So the real polarizability is also anisotropic:

$$\boldsymbol{\eta} = (\boldsymbol{\rho}_t - \boldsymbol{\rho}) * \mathrm{inv}(\boldsymbol{\rho}_t) \tag{12}$$

In FDIP, the amplitude and phase of complex resistivity at multi-frequency of the earth can be described by Cole-Cole relaxation models (Cole and Cole, 1941; Pelton et al., 1978). This equation is:

$$\rho(w) = \rho_0\left\{1 - m\left[1 - \frac{1}{1+(jw\tau)^c}\right]\right\} \tag{13}$$

The physical properties of these parameters ρ_0, m, τ, c can be referenced in (Luo and Zhang, 1998). When the subsurface is anisotropic, the Cole-Cole parameters can also be illustrated as a tensor, so complex resistivity response at different frequencies of the anisotropic medium can be calculated:

$$\boldsymbol{\rho}(w) = \boldsymbol{\rho}_0 \left\{ \mathrm{I} - \mathbf{m} * \left[\mathrm{I} - \mathrm{inv}(\mathbf{I} + (jw\boldsymbol{\tau})^{c}) \right] \right\} \quad (14)$$

where, I is an identity matrix, in addition, $\boldsymbol{\rho}_0, \mathbf{m}, \boldsymbol{\tau}$ are tensors and c is a scalar.

Numerical Examples

Verifying the numerical accuracy

Firstly, we used a two-layer vertical anisotropic resistivity model to verify the accuracy of the FVM method. **Figure 1** illustrates the two-layer model. Schlumberger sounding arrangement was used with potential electrodes MN=20 m, and the current electrodes AB ranged from 60 m to 6000 m. This two-layer vertical anisotropic model has an equivalent isotropic layered model with ρ_M and λh for first isotropic layer and 10 Ω m for the second half-space. **Figure 2** shows the results of analytic solution and numerical solution and relative error. From **Figure 2**, for the two-layer anisotropic model, the mean error was about 0.23% and max error was about 0.73%.

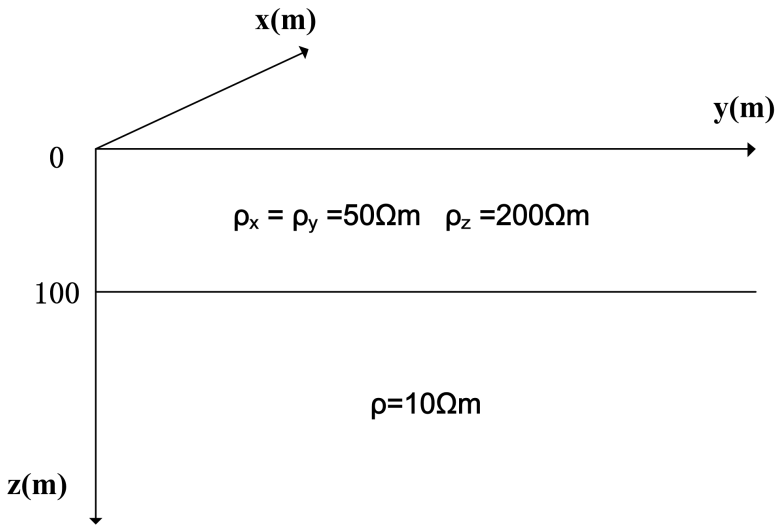

Figure 1: Sketch of a two-layer model consisting of a vertical anisotropic cover layer over an isotropic half-space

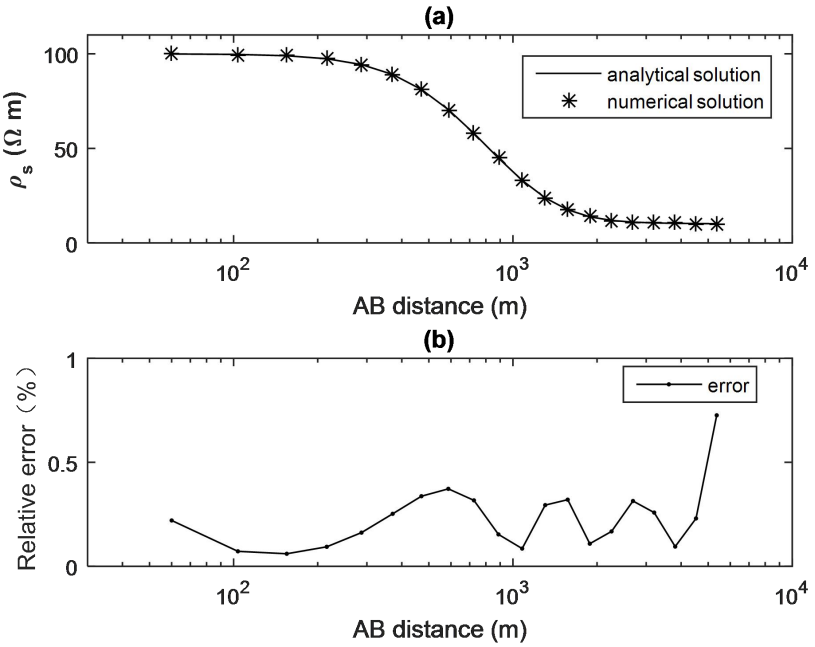

Figure 2: Apparent resistivity curve using Schlumberger sounding arrangement for a two-layer vertical anisotropic model: (a) analytical solution and numerical solution; (b) the relative error.

IP response for a horizontal anisotropic two-layer model

Subsequently, the TDIP and FDIP responses for a horizontal anisotropic two-layer model were studied. First, we calculated the TDIP response. **Figure 3** depicts the two-layer model. Two survey lines perpendicular to each other were arranged on the surface using the same sounding arrangement protocol as the former model. **Figure 4** shows the curves of apparent resistivity and apparent polarizability for the two directions.

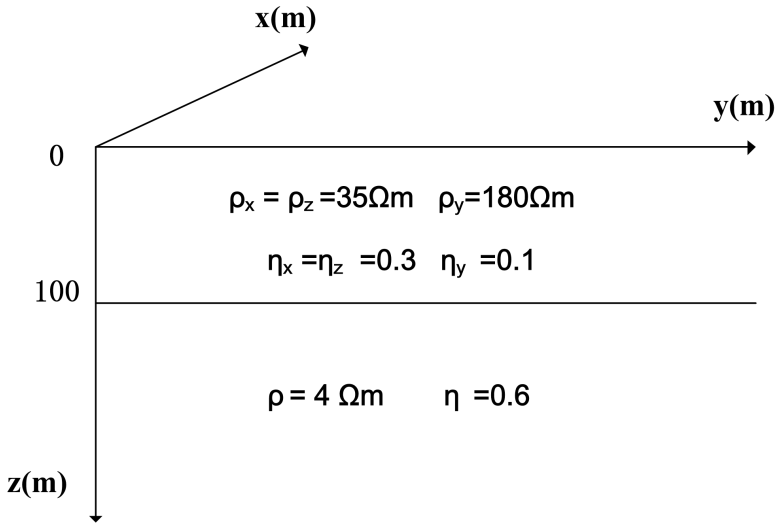

Figure 3: Sketch of a two-layer time domain induced polarization model consisting of a horizontal anisotropic cover layer over an isotropic half-space

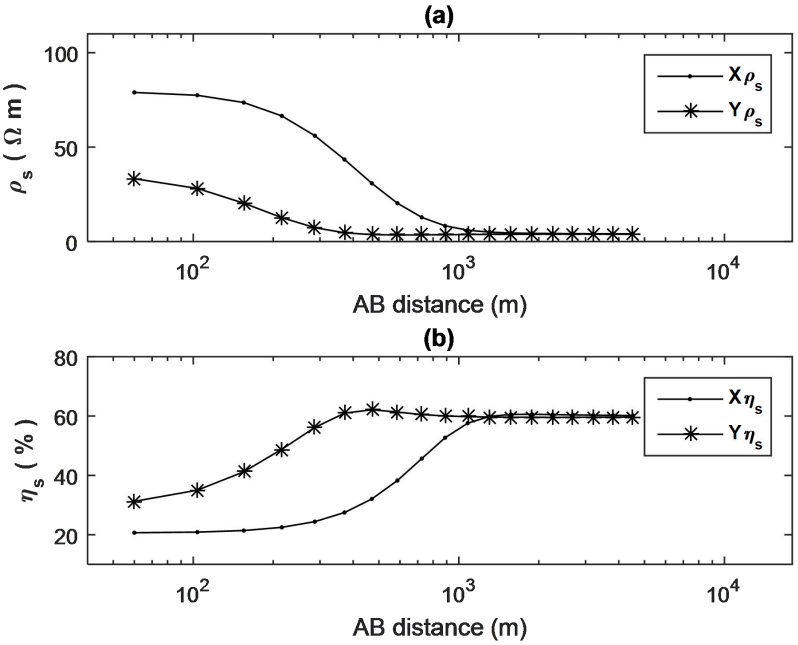

Figure 4: (a) Apparent resistivity curves using Schlumberger sounding arrangement for a two-layer time domain induced polarization model in two orthogonal measuring directions; (b) Apparent polarizability sounding curves in the two orthogonal measuring directions.

From **Figure 4**, the apparent resistivity and apparent polarizability differ in X direction and Y direction. When the survey line is in X direction, the apparent original resistivity trend to 79 Ω m and 4 Ω m at the two ends of the sounding curve respectively. In contrast, when the survey line is in Y direction, trend of the apparent original resistivity is 35 Ω m and 4 Ω m . The different phenomenon between the X direction and Y direction is called anisotropy paradox (Bhattacharya,1968), namely, in the first layer, apparent ρ_x^a trends to $\sqrt{\rho_x \rho_y}$ and apparent ρ_y^a .trend to ρ_x . However apparent polarizability in two directions trend to 0.2 and 0.3 respectively when the AB is small. The real polarizability is 0.3 and 0.1, so the apparent η_y^a trends to η_x , but η_x^a does not trend to $\sqrt{\eta_x \eta_y}$.

Then we calculated the FDIP response using Cole-Cole model. **Figure 5** illustrates the two-layer model. **Figure 6** shows the curves of apparent resistivity and apparent phase for the two directions.

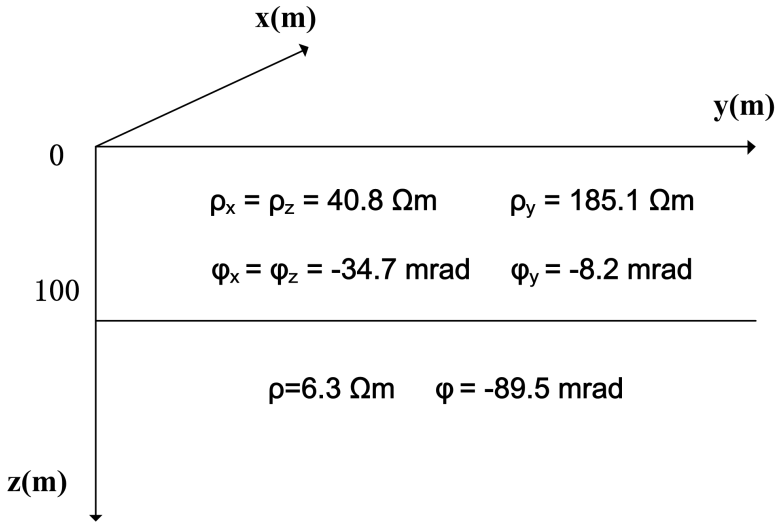

Figure 5: Sketch of a two-layer frequency domain induced polarization model consisting of a horizontal anisotropic cover layer over an isotropic half-space

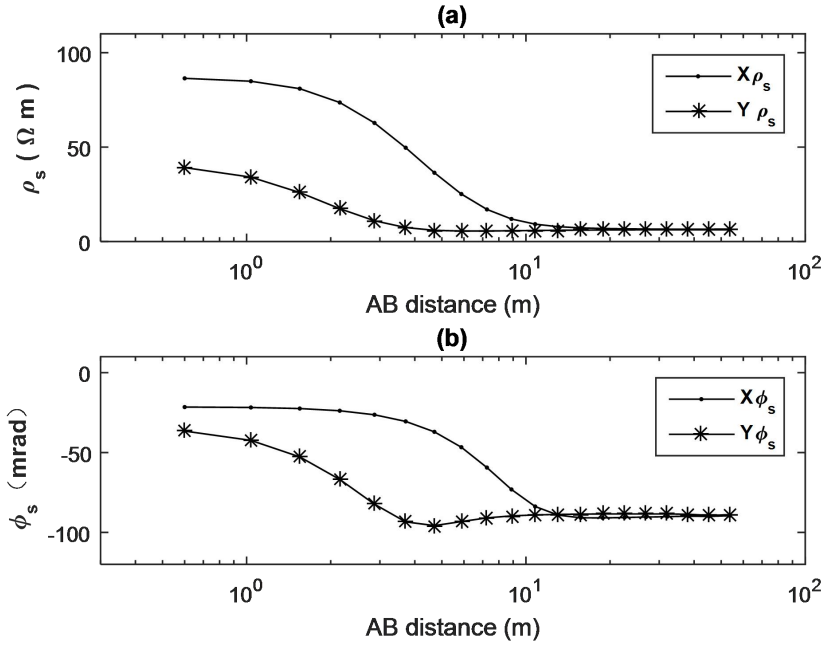

Figure 6: (a) Apparent resistivity curves using Schlumberger sounding arrangement for a two-layer frequency domain induced polarization model in two orthogonal measuring directions; (b) Apparent phase sounding curves in the two orthogonal measuring directions.

From **Figure 6,** when the current electrodes distance AB was small, apparent resistivity trends to 86.9 Ω m in X direction and 40.8 Ω m in Y direction. In addition, apparent phase trends to -21.45 mrad in X direction and -34.7 mrad in Y direction. These are also consistent with the anisotropy paradox, namely, apparent $\rho_x^a \to \sqrt{\rho_x \rho_y}$, apparent $\rho_y^a \to \rho_x$ and apparent $\varphi_x^a \to \frac{\varphi_x + \varphi_y}{2}$ t, apparent $\varphi_y^a \to \varphi_x$.

When the AB distance is large enough, apparent resistivity and phase in X and Y directions trend to $6.3\ \Omega\ \mathrm{m}$ and $-89.5\ \mathrm{mrad}$, which is the same as the real complex resistivity of the second isotropy layer.

IP response for a 3D cube in a horizontal anisotropic half-space

Then, the TDIP and FDIP of a 3D cube embedded in the horizontal anisotropic half-space was studied. First, we studied the TDIP response. **Figure 7** illustrates this 3D TDIP model parameters.

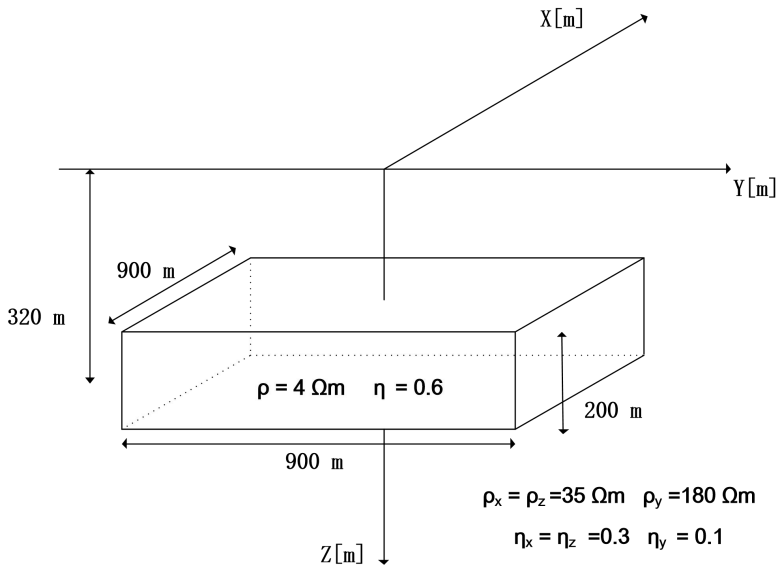

Figure 7: Sketch of a 3D cube time domain induced polarization model embed in a horizontal anisotropic subsurface half-space

In order to describe the 3 D model, 35 survey lines with 35 survey points per line were constructed in turn. Intermediate gradient array protocol was used for each survey line. The power supplying was in two directions X and Y and they are perpendicular to each other. The survey lines in two directions are shown in **Figure 8. Figure 9** shows contour maps of the apparent resistivity and apparent polarizability when survey lines are along X direction and Y direction separately.

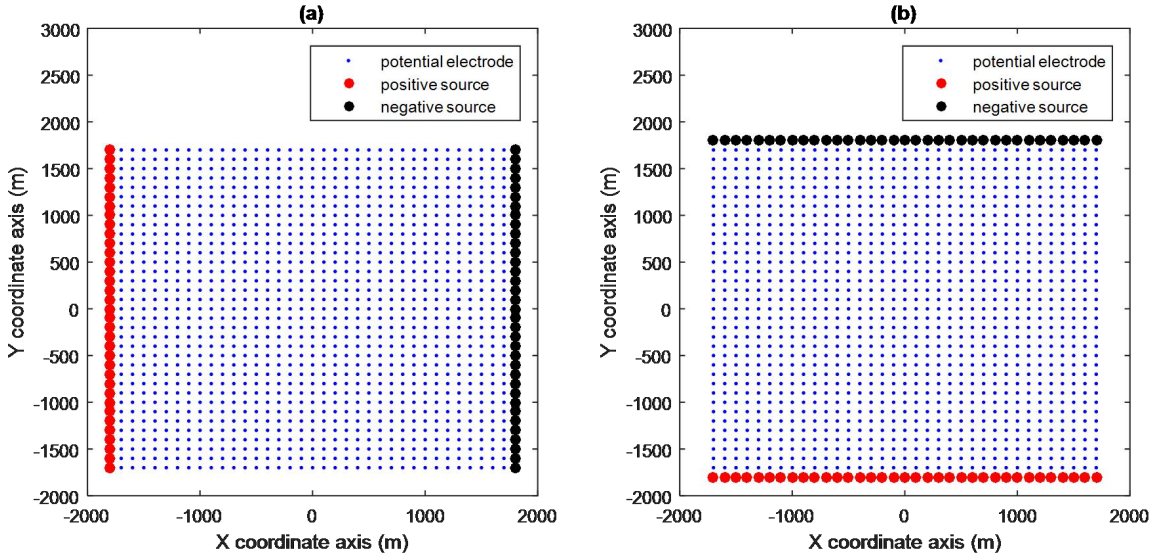

Figure 8: Layout diagram of 35 survey lines along the X direction (a) and Y direction (b) with 35 survey points in each line

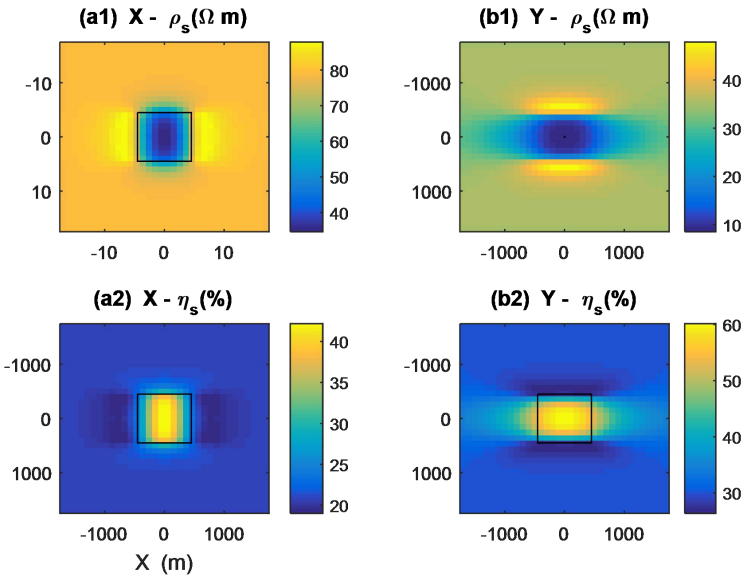

Figure 9: Contour maps of apparent parameters for a 3D cube time domain induced polarization model embed in a horizontal anisotropic subsurface half-space (the 35 survey lines are along X direction and Y direction separately using intermediate gradient array protocol; black rectangle represents location of the embedded cube):(a1) apparent resistivity for X survey lines; (a2) apparent polarizability for X survey lines; (b1) apparent resistivity for Y survey lines; (b2) apparent polarizability for Y survey lines;

From **Figure 9** we can see that the anomaly areas of the contour maps are consistent with the target cube location. The anomalies were compressed along the survey line. Because the 3D model is anisotropy, contour maps of the apparent parameters are not the same between X direction and Y direction. These should be taken account of in practical TDIP exploration.

Then, we studied the 3D FDIP response, **Figure 10** illustrates the 3D model parameters. **Figure 11** shows contour maps of the apparent resistivity and apparent phase when survey lines are along X direction and Y direction separately.

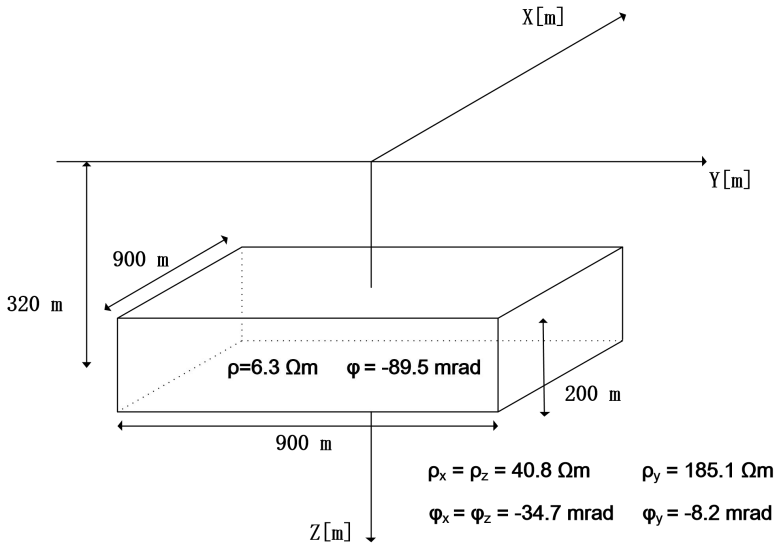

Figure 10: Sketch of a 3D cube frequency domain induced polarization model embed in a horizontal anisotropic subsurface half-space

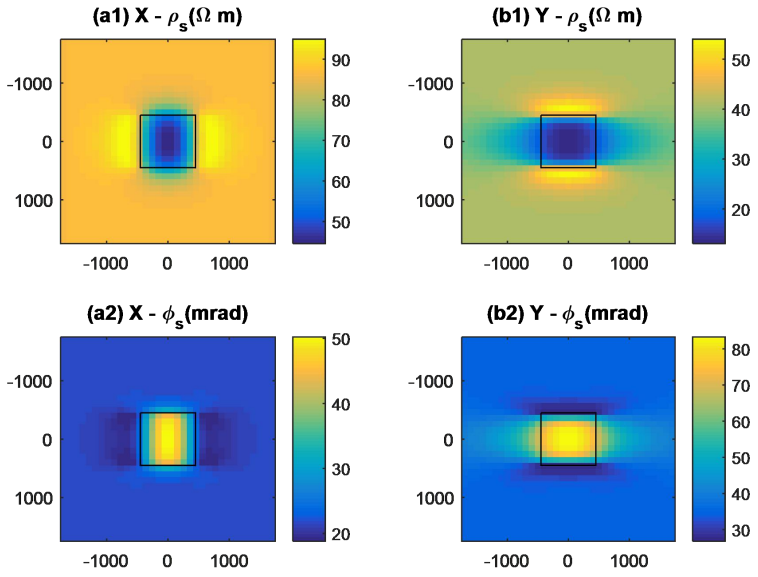

Figure 11: Contour maps of apparent complex resistivity for a 3D cube frequency domain induced polarization model embed in a horizontal anisotropic subsurface half-space (the 35 survey lines are along X direction and Y direction separately using intermediate gradient array protocol; black rectangle represents location of the embedded cube): (a1) apparent resistivity for X survey lines; (a2) apparent phase for X survey lines; (b1) apparent resistivity for Y survey lines; (b2) apparent phase for Y survey lines

From **Figure 11,** we can see that anomaly area of the apparent resistivity and phase in FDIP are also consistent with the target cube location. For the anisotropic subsurface, the apparent resistivity $\left|\rho_x^a\right|$

trends to $\sqrt{|\rho_x| * |\rho_y|}$ and the apparent phase φ_x^a trends to $(\varphi_x + \varphi_y)/2$ when the survey lines are along X direction. In contrast, the apparent resistivity $|\rho_y^a|$ trends to $|\rho_x|$ and the apparent phase φ_y^a trends to φ_x, when the survey lines are along Y direction. These also coincide with the anisotropy paradox.

IP response for a 3D horizontal anisotropic cube in an isotropic half-space

Finally, a 3D horizontal anisotropic cube in an isotropic half-space was studied. **Figure 12** shows the 3D TDIP model and FDIP model. **Figure 13** shows the two orthogonal survey lines in two directions X and Yon the surface. **Figure 14** shows curves of the calculated results of TDIP and FDIP models when survey lines are along X direction and Y direction separately.

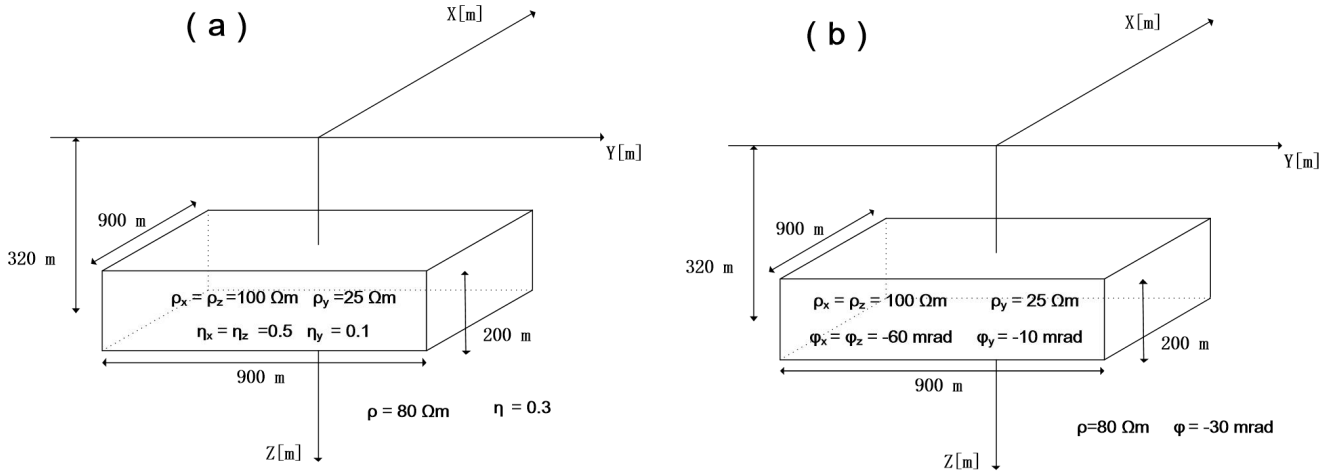

Figure 12: (a) Sketch of a 3D TDIP model in an isotropic half-space; (b) Sketch of a 3D FDIP model in an isotropic half-space;

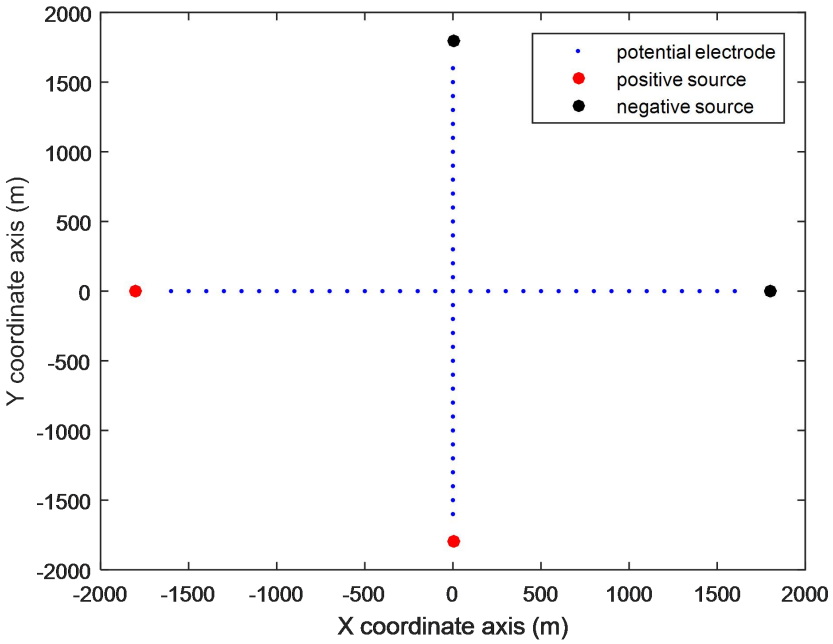

Figure 13: Two orthogonal survey lines in directions X and Y on the earth surface.

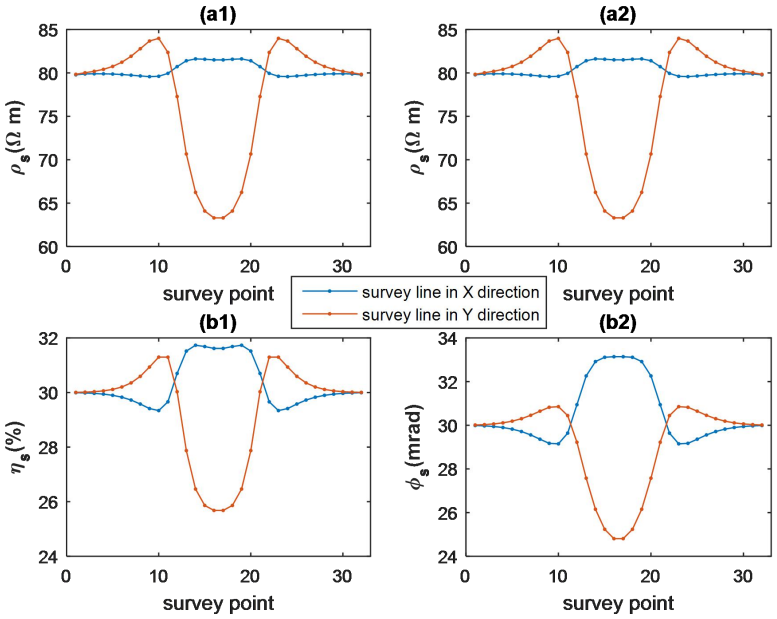

Figure 14: Simulated TDIP and FDIP results of a horizontal anisotropic cube embed in an isotropic half-space (two orthogonal survey lines were arranged): (a1) apparent resistivity in TDIP for the two survey lines; (b1) apparent polarizability in TDIP for the two survey lines; (a2) apparent resistivity in FDIP for the two survey lines; (b2) apparent phase in FDIP for the two survey lines.

From **Figure 14 (a1)** and **(b1),** for the TDIP, there is a high-resistivity and high-polarizability anomaly in the X survey line, however, there is a low-resistivity and low-polarizability anomaly in the Y survey line. From **Figure 14 (a2)** and **(b2),** For the FDIP, there is a high-resistivity and high-phase anomaly in the X survey line, however, there is a low-resistivity and low-phase anomaly in the Y survey line. So the apparent parameters of the 3D model is complex because of the anisotropy, which should be taken into account of in the practical IP exploration.

Conclusion and Discussion

In this paper, we modeled and analyzed the 3D time domain induced polarization (TDIP) and frequency domain induced polarization (FDIP) response in the anisotropic conductive subsurface using finite volume method (FVM). The following conclusions can be obtained: Finite volume method can be used to model the 3D resistivity response. Based on equivalent resistivity and Cole-Cole model respectively, TDIP and FDIP response can be calculated in anisotropic conductive subsurface. For TDIP, apparent resistivity also conforms to the anisotropy paradox, and apparent polarizability can be calculated using apparent original and equivalent resistivity. For FDIP, apparent complex resistivity is also consistent with this phenomenon. For 3D model, resistivity and induced polarization response of the anisotropic medium are quite complex and there are even no reasonable interpretation for some abnormal phenomenon at present. IP response in arbitrary anisotropy medium will also be studied further based on the anisotropy and coordinates rotation of the survey zone.

References

Kenkel, J., Hördt, A., Kemna, A., 2012, 2D modelling of induced polarization data with anisotropic

complex conductivities. Near Surface Geophysics 10(6), 533-544.

Kenkel, J., Martin, R., Kemna, A., 2013, Anisotropic Inversion of Induced Polarization (IP) Data. Near Surface Geoscience 2013-19th EAGE European, Meeting of Environmental and Engineering Geophysics.

Kenkel, J., Hördt, A., Kemna, A., 2014, Anisotropic complex conductivity inversion. Third International Workshop on Induced Polarization, Oleron Island,France.

Liu, W., Chen R., Wu, H., Qiu, J., Yao, H., Shen, R., Ren, Q., Chang, F., Zeng, P. and Luo, W., 2015, High precision FDIP exploration in productive mine with strong EM interference. Symposium on the Application of Geophysics to Engineering and Environmental Problems 2015, 65-73. doi: 10.4133/SAGEEP.28-008.

Liu, W, Chen, R., Cai, H. and Luo, W., 2016, Robust statistical methods for impulse noise suppressing of spread Spectrum induced polarization data, with application to a mine site, Gansu Province, China. Journal of Applied Geophysics, (available online) 1-11. doi:10.1016/j.jappgeo.2016.04.020.

Luo, Y., Zhang, G., 1998, Theory and Application of Spectral Induced Polarization. SEG Books.

Winchen, T., Kemna A., Vereecken H. and Huisman J.A., 2009, Characterization of bimodal facies distributions using effective anisotropic complex resistivity: A 2D numerical study based on Cole-Cole models. Geophysics 74, A19–A22.

Xi, X., Yang, H., He, L. and Chen, R., 2013, Chromite mapping using induced polarization method based on spread spectrum technology. Symposium on the Application of Geophysics to Engineering and Environmental Problems 2013, 13-19. doi: 10.4133/sageep2013-015.1.

Xi, X., Yang H., Zhao, X. and Chen, R., 2014, Large-scale distributed 2D/3D FDIP system based on ZigBee network and GPS. Symposium on the Application of Geophysics to Engineering and Environmental Problems 2014, 130-139. doi: 10.4133/SAGEEP.27-055.

Zhdanov, M., Alexander, Gribenko, Vladimir, Burtman, 2008, Anisotropy of induced polarization in the context of the generalized effective-medium theory. 2008 SEG Annual Meeting, Society of Exploration Geophysicists.